SEMICONDUCTOR CAMERA FOR DETECTION OF SMALL TUMORS

A. E. Profio and Z. H. Cho

University of California, Los Angeles, California

Early detection of small tumors (approximately 3 mm) with only a moderate uptake ratio is often difficult because of poor statistics and a small signal-to-background ratio. The detection capability of a germanium semiconductor camera is analyzed to show that a very large number of counts is required even when the spatial resolution is matched to the size of the tumor. A potential enhancement of statistics using the tissue-scattered gamma rays is discussed based on the superior energy resolution of the semiconductor.

Early detection of tumors while they are still small (a few millimeters diameter) and before they have metastasized is a difficult task for existing sodium iodide scintillation cameras. The spatial resolution of these devices is typically on the order of 1 cm and sensitivity is relatively low (geometric efficiency about 10^{-4}). Total activity in the tumor is small; hence statistics in the counts are poor. Detection and localization of a "hotspot" or tumor with increased uptake of a radionuclide is made more difficult by the background radioactivity remaining in the blood or surrounding tissue. In fact, the statistical precision in the signal and background counts is a limiting condition on detectability. An improvement in detectability would have great rewards medically.

Semiconductor arrays of either lithium-drifted germanium (*1*) or high-purity germanium (*2*) are being fabricated into cameras for possible application to nuclear medicine. A typical device consists of a slab 5 mm thick, divided electrically into a matrix with elements a few square millimeters in area. The X and Y coordinates of a count in a given element are read out as coincident signal pulses on appropriate electrodes while the total energy deposited is obtained from the sum. Spatial resolution is better than in the standard sodium iodide scintillator and the semiconductor has excellent energy resolution for low-energy gamma rays, about 4 keV (FWHM) at 140 keV. A possible arrangement of tumor, scattering medium (tissue), multiple parallel-hole collimator, and high-purity germanium detector is shown in Fig. 1.

The purpose of this paper is to define the optimum size for the semiconductor detector element, to investigate the statistical precision required for identification of a "hot" tumor above blood background, and to suggest a possible enhancement of statistics by utilizing the gamma rays which are Compton-scattered in the surrounding tissue. The last exploits the energy resolution of the semiconductor; the resolution of a sodium iodide scintillation camera would not be adequate.

Received Dec. 6, 1973; revision accepted Aug. 15, 1974.

For reprints contact: A. E. Profio, Dept. of Chemical and Nuclear Engineering, University of California, Santa Barbara, Calif. 93106.

STATISTICS

Statistical considerations in detectability of small regions of differing activity concentration have been discussed before, e.g., by Beck (*3*). We have reformulated the problem in a different way to show explicitly the dependence of detectability on the dimensions of the target region and detector-collimator element size a_D (or effective spatial resolution) as well as on the uptake ratio $U = I_t/I_0$ where I_t is the activity per unit volume in the tumor (γ/sec-cm^3) and I_0 is the activity per unit volume in the tissue.

Let us consider a small tumor represented as a cube a_t cm on a side where a_t is small compared with either the total thickness H of the surrounding emitting tissue or the depth d at which the tumor is supposed to be embedded (Fig. 1). We can account for attenuation by defining an effective thickness of tumor $h' = a_t\, e^{-\mu d}$ and effective thickness of tissue $H'\text{-}(1 - e^{-\mu H})/\mu$, where μ is the linear attenuation coefficient.

Then the counts C_0 from the nontarget volume (when the tumor is absent) is

$$C_0 = (a_D^2\, H' I_0) G\eta T \qquad (1)$$

where G is a geometry factor, η (counts/γ-incident) is the detection efficiency, and T (sec) is the counting time. The count C_t contributed from the tumor is

$$C_t = (a_t^2\, I_t h') G\eta T \qquad (2)$$

Hence the total count C_1 over the target

$$C_1 = C_0 + C_t - (a_t^3\, I_0 e^{-\mu d}) G\eta T \qquad (3a)$$

or

$$\cong C_0 + C_t \qquad (3b)$$

when a_t is negligible compared with H. We assume also that $a_t \leq a_D$ so that all of the tumor volume contributes to C_t. The expression is easily modified if $a_t > a_D$.

Detectability in a statistics-limited situation depends on obtaining a significant target-to-nontarget count ratio which from Eqs. 1–3 may be written

$$\frac{C_1}{C_0} = 1 + \frac{C_t}{C_0} = 1 + \left(\frac{a_t}{a_D}\right)^2 \frac{h'}{H'} U \qquad (4)$$

Detectability is improved by a large uptake ratio, relatively thin surrounding tissue (particularly tissue containing the radionuclide), and by making the collimator aperture and detector element size comparable to tumor dimensions (approximately a few millimeters or less) or in general by matching the spatial resolution of the camera to the size of the tumor. The reason, of course, is that when a_D (or an equivalent spatial resolution length) exceeds a_t, all

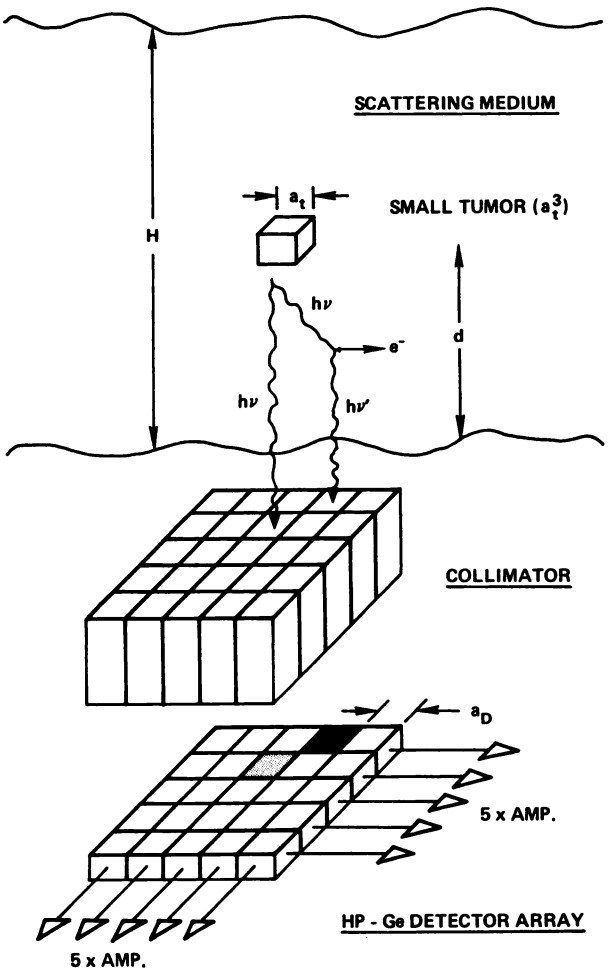

FIG. 1. Small tumor detection system with semiconductor detector array.

of the tumor contributes already but C_0 continues to increase as more of the background tissue is included in the field of view. Because we are interested in detecting tumors about 3 mm in diam, we propose making the semiconductor detector element and the collimator aperture about 3 mm × 3 mm.

It is interesting to evaluate the required number of counts, C_0 or C_1, as a function of a_t/a_D, h'/H', and U. Thus the physician should be able to estimate the number of counts which must be accumulated to detect a certain size tumor or the minimum size tumor one may be able to detect under given conditions. The usual criterion is a 95% confidence level, requiring that the means differ by at least 2 s.d.; hence

$$C_1 - C_0 \geq 2\,(C_1 + C_0)^{1/2} \qquad (5)$$

where Poisson statistics have been assumed. Near the limit of detectability, $C_1 \approx C_0$ hence we require

$$C_0 \geq \left[\frac{2.8}{\left(\frac{a_t}{a_D}\right)^2 \frac{h'}{H'} U}\right]^2 \qquad (6)$$

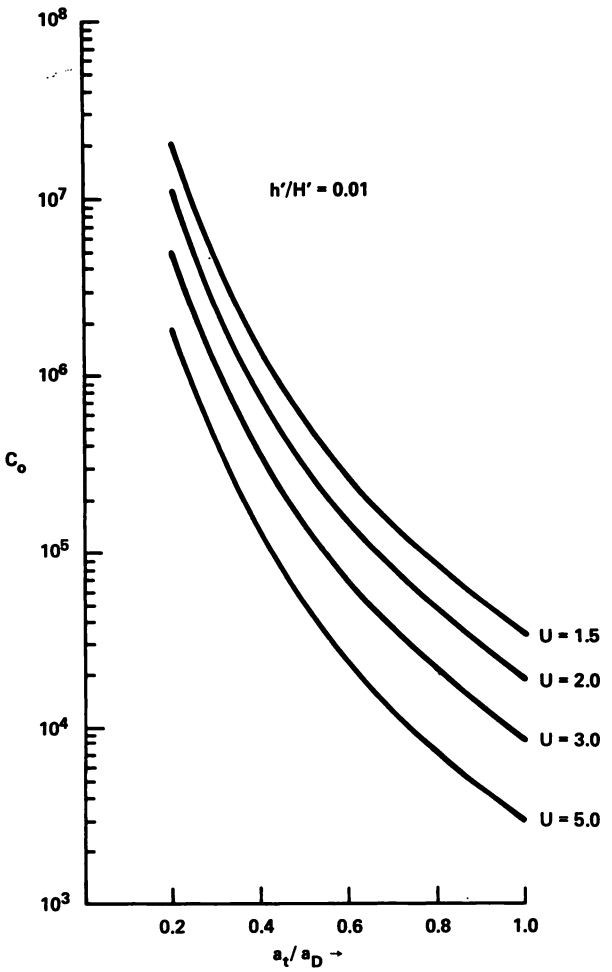

FIG. 2. Required counts (C_0) for small tumor detection as function of tumor-to-detector size ratio a_t/a_D.

The number of counts required is plotted in Fig. 2 as a function of a_t/a_D, for various values of the uptake ratio, at $h'/H' = 0.01$. The number may be scaled as $(h'/H')^{-2}$. Equation 6 breaks down for U near unity because the displacement correction term in Eq. 3a has been neglected and C_0 and C_1 assumed equal in computing the variance. When the activity concentrations are equal and $U = 1$, the tumor cannot be distinguished from the surrounding tissue no matter how good the statistics.

Detectability is always enhanced by large C_1 and C_0 hence by a dose-efficient tracer, large intrinsic efficiency of the detector, and large geometry factor for the collimator. A useful tracer is ^{99m}Tc (140-keV gamma ray). Assume a 3-mm-size tumor embedded at the center of a 10-cm thick tissue region (hence $d = 5$ cm, $H = 10$ cm), an uptake ratio of two, and $\mu = 0.15$ cm^{-1}. By our theory, we need to accumulate 2,600 counts per element, or 2.9×10^4 c/cm^2, to detect a 3-mm-diam tumor with $a_t = a_D$. If the aperture is not matched but is fixed at $a_D =$ 1 cm, it would take 3.2×10^5 counts/cm^2 to detect a 3-mm-diam tumor. In present practice with sodium iodide scintillation cameras, 10^2–10^3 counts/cm^2 is typical which means only large tumors can be detected unless h'/H' is favorable or a radioisotope is employed with a particularly favorable dose efficiency (maximum I_t per rad) and uptake ratio or the counting time is very long.

EFFICIENCY

The intrinsic efficiency of the germanium detector, 5–10 mm thick, is less than that of a typical 1.25-cm thick sodium iodide detector but is adequate below 150 keV.

It is most important to achieve a large geometric efficiency. This presents a problem when the aperture a_D is small because with a parallel-hole collimator, the uncollided gamma rays from a near point source interact in only one detector element and the distance from detector to tumor is necessarily many times a_D. Thus the fractional solid angle subtended by the detector element (*4*) is only about 10^{-4}. We have investigated another possibility, i.e., to count the scattered gamma rays as well as the uncollided ones. As seen in Fig. 1, gamma rays are scattered into all elements of the detector array and for the conditions assumed, more than half the gamma rays emerging have been scattered.

SCATTERED RADIATION

Normally the counts from scattered gamma rays are rejected by energy discrimination. Beck, et al (*5,6*) have suggested accepting some of the scattered gamma ray counts on the theory that the increase in counts may compensate for the smearing in spatial resolution. These ideas have been employed to select "optimum" radionuclide gamma ray energies and settings of the pulse-amplitude analyzer. The semiconductor offers more flexibility because of its good energy resolution. However, the enhancement seems limited to definition of large objects which does not aid the problem of detecting small tumors.

We have explored a different approach, i.e., to use the unique energy-angle relationship in single Compton scattering to work back to the position of the source. Figure 3 diagrams the scattering and collimation geometry. The energy E_0 (keV) of the monoenergetic source is known, hence the energy after scattering is obtained from the usual expression

$$E = \frac{E_0}{1 + (E_0/511)(1 - \cos\theta)} \qquad (7)$$

and is measured by ionization in the semiconductor. The angle of incidence is defined by the collimator to essentially 90 deg. Therefore, the angle of scattering

can be measured. For E_0 equal to 140 keV and an energy resolution of about 5 keV, the counts can be sorted into 10 angular intervals of scattering as listed in Table 1.

Once the scattered energy is measured, the linear attenuation coefficient $\mu(cm^{-1})$ and the differential scattering coefficient $\mu_s(E_0, \theta)cm^{-1}$ steradian^{-1} are known, given the composition of the scattering medium. The values listed in Table 1 apply to water or soft tissue. Even if the exact composition is unknown, the intensity of scattered radiation can be related reasonably accurately to the intensity of the uncollided radiation.

The number of photons scattered into a detector element from volume element dV per source photon is

$$dN_1 = \frac{e^{-\mu(E_0)r_1}}{4\pi r_1^2} \frac{e^{-\mu(E)r_2}}{(r_2 + L)^2} \mu_s(E_0, \theta) a_D^2 \, dV \quad (8)$$

where $r_1 = b \csc \theta$ and $r_2 = d - b \cot \theta$. If d and b (e.g., the hole-to-hole spacing) are assumed, the number of single-scattered photons incident on the detector can be evaluated by integrating Eq. 8 over the volume.

An approximate trial calculation has been made for d = 5 cm, L = 3 cm, scattering from 0 deg to 90 deg only, and integrating only from 0 to b = 5 cm. Shading by the collimator septa was neglected. The scattered number is 4.6×10^{-5} gamma rays incident per gamma ray emitted, compared with the uncollided number 5.3×10^{-5}. The counts are obtained by multiplying by the intrinsic efficiency. Considering that the efficiency is larger for the low-energy scattered gamma rays and only a portion of the scattering volume has been included, we conclude that the counts from scattered gamma rays should be comparable to the counts from uncollided gamma rays.

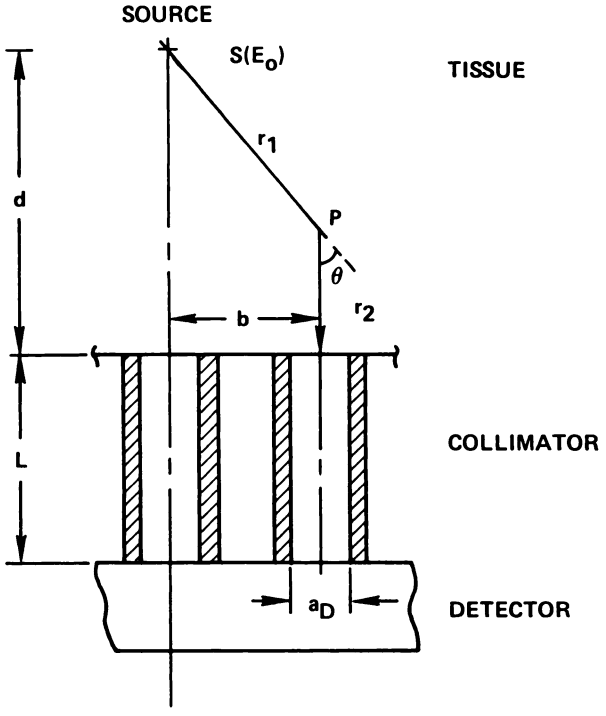

FIG. 3. Single scatter geometry.

TABLE 1. SCATTERING PARAMETERS

Interval	E (keV)	θ (deg)	μ (cm^{-1})	μ_s (cm^{-1}sr^{-1})
1	140	0	0.153	0.026
2	135	30	0.155	0.022
3	130	45	0.157	0.017
4	125	55	0.158	0.016
5	120	66	0.160	0.012
6	115	79	0.162	0.010
7	110	90	0.164	0.009
8	105	103	0.166	0.009
9	100	117	0.167	0.009
10	95	137	0.169	0.011
	90	180	0.170	0.013

If the position of the tumor is suspected, the scattered counts can be corrected for attenuation and the differential scattering probability by the relationship of Eq. 8 and added to the counts from the uncollided photons in the detector element aligned on the tumor. Another way to make use of the scattered photons is to determine the depth of a hot spot (with general background subtracted) from the smallest angle-of-scatter, hence greatest energy observed at a given radius. We have in fact located a point source (in air) from the angle of scatter in a thin slab of plastic placed over the source. In such a simplified situation, the position of scattering is defined as well as the angle and the source can be located by straightforward triangulation.

In the more general situation, scattering can occur at any depth. The detected energy and the collimation define the scattering angle but the source can be anywhere on a cone of half-angle θ. Thus we are faced with an unfolding problem to reconstruct the three-dimensional spatial distribution of radioactivity from the observed counts as a function of position (detector element) and energy. Unfolding of radioisotope emission distributions with corrections for attenuation has been carried out already using multiple projections (*7–9*). Unfolding can also be accomplished by iterative least-squares technique (*10*), given the response matrix, i.e., the pulse-height spectrum (counting rate versus energy) as a function of radius b and depth d for a unit-strength monoenergetic point source. The response matrix applies to

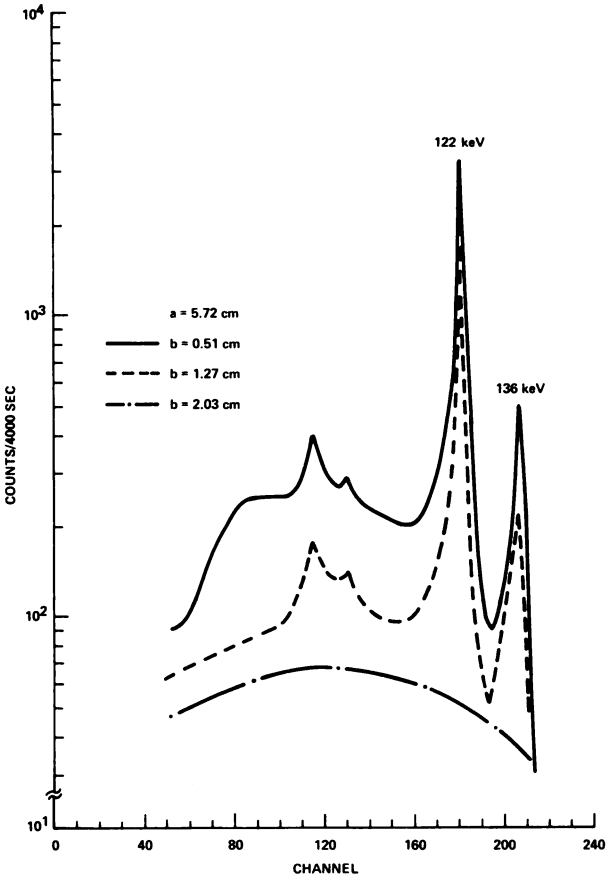

FIG. 4. Response spectra for ^{57}Co in water.

a specific source energy, collimator and detector arrangement, and scattering medium. It can be calculated by the Monte Carlo technique or better measured. Multiple-scattered photons, which we have neglected thus far, are included in the response matrix.

We have measured the response matrix for a 5.4 μCi ^{57}Co source in water (30-cm cube contained in a plastic vessel) by traversing the source at various depths across a single-hole lead collimator aligned on a 30-cm^3 Ge(Li) detector. The collimator hole was cylindrical, 0.32 cm in diam and 1.19 cm long, spaced 1.51 cm from the front surface of the germanium detector. Examples of measured pulse-height distributions, background-subtracted and smoothed, are given in Fig. 4. Normalized to unit activity and interpolated in depth and radius, the set of such spectra constitutes a response matrix. With a semiconductor camera, of course, the response matrix could be measured by moving the source in depth only.

CONCLUSION

Statistical analysis shows that detection of small tumors embedded in a region of background radioactivity will require matching of camera resolution to tumor size and orders-of-magnitude improvement in overall detection efficiency. A possible method of improving efficiency is to utilize the tissue-scattered photons as well as the uncollided photons. The energy resolution of a semiconductor detector along with a parallel-hole collimator may be exploited to define the scattering angle. The general problem of reconstructing an unknown three-dimensional distribution of radioactivity will require unfolding from the observed counts as a function of energy and position, e.g., utilizing a measured or calculated response matrix for a point source.

REFERENCES

1. PARKER RB, GUNNERSEN EM, WANKLING JL, et al: A semiconductor gamma camera with quantitative output. In *Medical Radioisotope Scintigraphy*, vol 1, Vienna, IAEA, 1969, p 71

2. DETKO JE: Performance characteristics of an ultra pure germanium gamma camera. *Radiology* 104: 431–433, 1972

3. BECK RN: A theory of radioisotope scanning systems. In *Medical Radioisotope Scanning*, vol 1, Vienna, IAEA, 1964, p 35

4. BROWNELL GL: Theory of radioisotope scanning. In *Medical Radioisotope Scanning*, vol 1, Vienna, IAEA, 1964, p 3

5. BECK RN, SCHUH MW, COHEN TD, et al: Effects of scattered radiation on scintillation detector response. In *Medical Radioisotope Scintigraphy*, vol 1, Vienna, IAEA, 1969, p 595

6. BECK RN, ZIMMER LT, CHARLESTON B, et al: A theory of optimum utilization of all detected radiation. In *Semiconductor Detectors in Medicine*, CONF 73-0321, Oak Ridge, USAEC, 1973, pp 87–106

7. BUDINGER TF, GULBERG GT: Three-dimensional reconstruction in nuclear medicine imaging. *IEEE Trans Nucl Sci* NS-21: No. 3, pp 2–20

8. CHO ZH: General views on 3-D image reconstruction and computerized transverse axial tomography. *IEEE Trans Nucl Sci* NS-21: No. 3, pp 44–71

9. GORDON R: A tutorial on ART (algebraic reconstruction techniques). *IEEE Trans Nucl Sci* NS-21: No. 3, pp. 78–93

10. KENDRICK H, SPERLING SM: *Introduction to Principles and Use of the Ferdor Unfolding Code.* Gulf Radiation Technology Report GA-9882, 1970